

POWER QUALITY IMPROVEMENT OF THREE-PHASE  
AC-DC POWER CONVERSION BY  
DISCONTINUOUS MODE "DITHER"-RECTIFIERS

JOHANN W. KOLAR, HANS ERTL, FRANZ C. ZACH  
Technical University Vienna, Power Electronics Section,  
Gußhausstraße 27, Vienna, AUSTRIA

Phone: (int)43 222 58801-3886 Fax: (int)43 222 5052666

Abstract

The main topic of this paper is the analysis of three-phase unidirectional AC/DC power converters and the improvement of their power conversion operation.

By distributing the energy storage device on the input side to the phases of the three-phase mains and subsequent bridge rectification well known DC/DC converters are extended to AC/DC converters with three-phase input. If the systems are operated in discontinuous mode, the peak values of the input phase currents or voltages within a pulse period show an envelope which is proportional to the mains phase voltages. This assumes on- or off-intervals of the power switch which are time-constant over the fundamental period and given by the output voltage control circuit. After filtering the high-frequency components of the input quantities, approximately sinusoidal mains currents result. Thereby a substantial reduction of the influence on the mains as compared to the conventional line-commutated rectification is given. The phase shift between mains phase voltage and current is determined by the input filter and is limited to small values due to the system switching frequency being substantially higher than the mains frequency.

The basic function of the derived new class of three-phase rectifier circuits is described by using the example of a discontinuous inductor current boost and of a discontinuous input capacitor voltage buck rectifier. The latter circuit follows from dual transformation of the former circuit. Furthermore, the current shapes resulting in dependency on the voltage transformation ratio, the spectrum of these currents and guidelines for filter dimensioning are discussed. Finally, further topologies of three-phase unidirectional pulse rectifiers are given.

## 1 Introduction

For coupling the mains with the capacitively buffered voltage DC link of low and medium power electronic systems uncontrolled three-phase bridge rectifiers are used in most cases today. The mains behavior of this concept is characterized by the occurrence of low-frequency mains current harmonics with high amplitudes. This is true especially for direct mains connection and for discontinuous DC current. It is known that current harmonics lead to a distortion of the voltages due to the corresponding voltage drops caused by the inner mains impedance. Therefore, the power

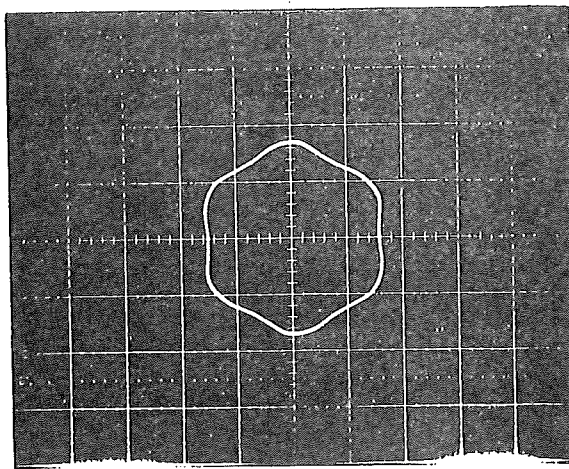


**Fig.1:** Trajectory of the space vector of the phase voltages measured on the 380V AC mains of the Electrotechnical Building of the TU-Vienna. Mains with a highly non-linear load component (office machines, computer systems etc.).

companies usually give regulations and recommendations especially for low-frequency harmonics in order to minimize the influence of other loads and systems supplied by the same mains. This gives the motivation to stress more and more the field of EMI (electromagnetic influence), namely the minimization of harmonics in the mains and the optimization of the power factor. Concerning PWM converter systems with voltage DC link the main effort so far has been lying in the area of power circuit design and control of the power flow of the load side.

In connection with the high harmonic content of public mains caused by two-pulse rectifiers of mass-production circuits (cf. Fig.1, [1]) especially the 5<sup>th</sup> mains harmonic is of interest for three-phase rectifiers. As shown in [2], this current harmonic shows a phase angle which is largely independent of the load and the mains reactance. Therefore, for assessing the influences on the mains of several three-phase diode bridges one has to consider the arithmetic sum of their 5<sup>th</sup> harmonics. A reduction of the resulting harmonic influence of the mains by superposition of harmonics with different phase angles is only given for higher order harmonics.

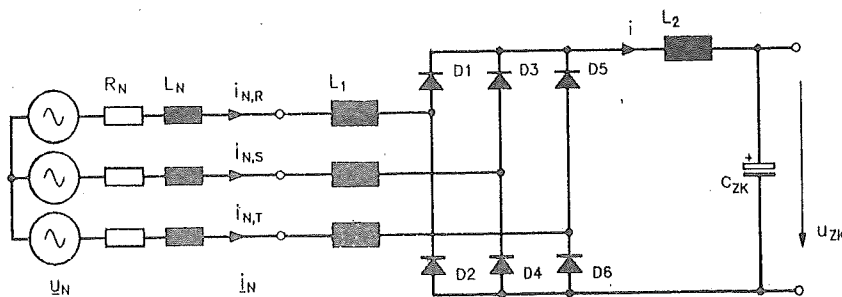


**Fig.2:** Basic power circuit of an uncontrolled three-phase (B6) bridge rectifier with inductive smoothing located on the AC side and on the DC side (inductances  $L_1$  and  $L_2$ ); output voltage  $u_{ZK}$  is buffered capacitively.  $R_N$  and  $L_N$  represent the equivalent circuit of the inner impedance of the supplying mains.

A reduction of the mains influence can be achieved in the simplest way by inductors in the mains connections or by a smoothing inductor connected on the DC side. This leads to the basic power circuit of an uncontrolled three-phase bridge circuit (B6) as shown in Fig.2. For smoothing on the DC side (cf. Fig.3) one can achieve a higher reduction of the 5<sup>th</sup> and 7<sup>th</sup> harmonic as compared to the same smoothing effort ( $3L_1 = L_2$ ) on the AC side (cf. Fig.4). This can be seen also from the reduced DC current ripple and, especially clearly, from a comparison of the trajectories of the mains currents space vectors (cf. Fig.5, [3]).

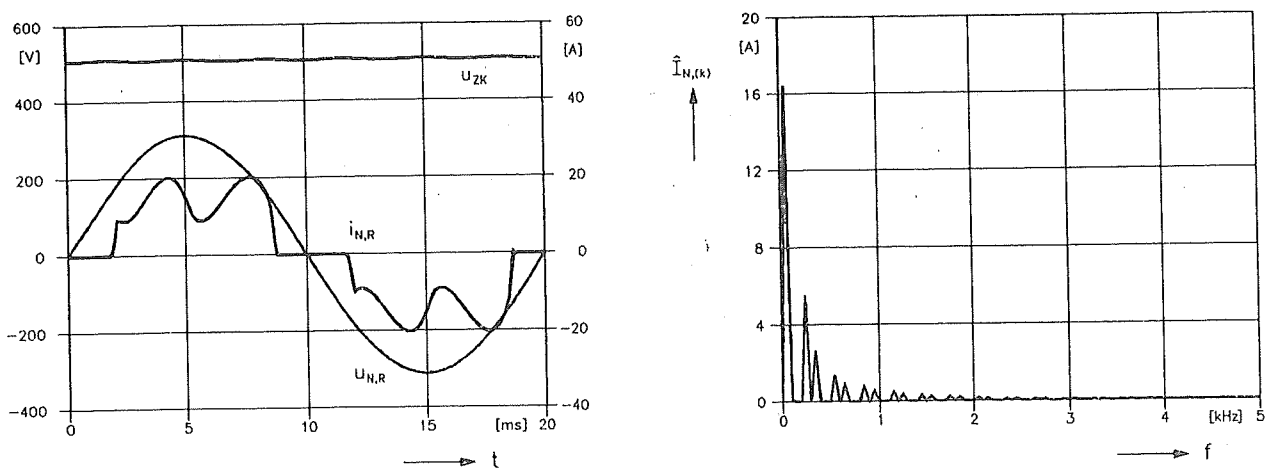


**Fig.3:** Simulation of the operating behavior of a B6-circuit (cf. Fig.2) for inductive smoothing on the DC side only; left: time behavior of a phase voltage, of the corresponding phase current and of the DC link voltage; right: spectrum of the phase current; parameters: output power  $P_L=7.5\text{kW}$ ,  $C_{ZK}=1.75\text{mF}$ ,  $L_1=0$ ,  $L_2=2.4\text{mH}$ ,  $R_N = 0.1\Omega$ ,  $L_N=0.4\text{mH}$ .

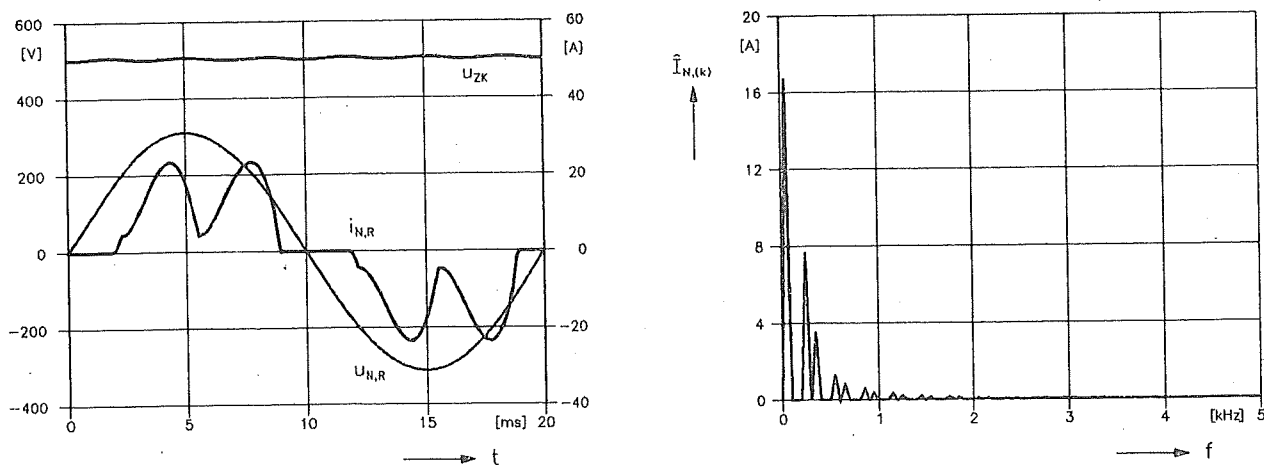


**Fig.4:** Simulation of the operating behavior of a B6-circuit (cf. Fig.2) for inductive smoothing on the AC side only; left: time behavior of a phase voltage, of the corresponding phase current and of the DC link voltage; right: spectrum of the phase current; parameters: output power  $P_L=7.5\text{kW}$ ,  $C_{ZK}=1.75\text{mF}$ ,  $L_1=0.8\text{mH}$ ,  $L_2=0$ ,  $R_N = 0.1\Omega$ ,  $L'_N=0.4\text{mH}$ .

Besides loading the mains by low-frequency current harmonics a basic disadvantage of uncontrolled rectifiers is given by the dependency of the DC link voltage on the mains voltage. This means that mains voltage tolerances have immediate influence on the dimensioning of the load side converter.

The problems discussed so far regarding the application of uncontrolled three-phase bridge circuits are the starting point of this paper. Basically, the minimization of the influences on the mains caused by diode bridges has to be performed via linearization of the nonlinear characteristic of the converter system (cf. Fig.6). The characteristic of an ideal linear rectifier system (which draws purely sinusoidal currents from the mains being in phase with the mains voltages) is given in Fig.6 as conductance line G.

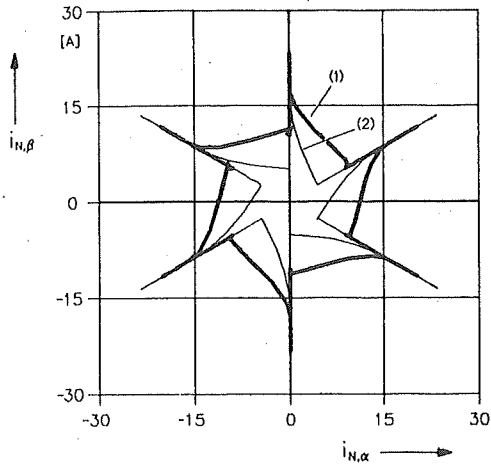


**Fig.5:** Trajectories of the current space vectors of a B6-circuit (cf. Fig.2) for inductive smoothing on the DC side (1) or on the AC side (2). Parameters as in Figs.3 and 4.

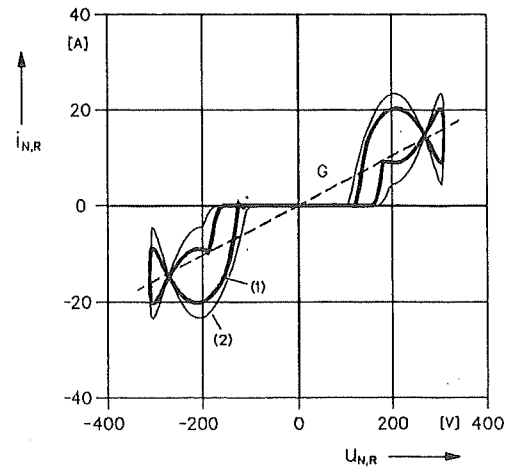


**Fig.6:** Dynamic current to voltage characteristics of a B6-circuit (cf. Fig.2) for inductive smoothing on the DC side (1) or on the AC side (2). Parameters as in Figs.3 and 4. Conductance line G: characteristic of a linear load with equal power consumption.

According to the theory of nonlinear control, a linearization of nonlinear systems can be achieved by a high-frequency (dither) signal superimposed on the system input signal. This principle, as proposed for single-phase converters in [4] is extended in this paper and transferred to three-phase systems.

By periodic high-frequency modulation of the DC side voltage (voltage dither) or of the DC side current (current dither) by a turn-off power semiconductor a power flow between the mains side and the DC side of a three-phase diode bridge is made possible within each pulse period. This means, that the power flow is continuous over the fundamental period. The high pulse currents being characteristic for simple diode rectifiers are avoided. In analogy to the definitions of the controls area, these pulse rectifier systems shall be called *dither-rectifier* systems.

For further concepts of pulse converter systems with low influence on the mains one has to refer to the literature, especially to [5]–[9].

In the following the basic operating principle of this new class of converter systems is described for the example of a voltage-dither boost and a current-dither buck rectifier. According to the classical theory of power electronics these circuits are to be called discontinuous input current boost rectifier or discontinuous input capacitor voltage buck rectifier, respectively, according to the current and voltage generation on the AC side. For the sake of brevity we want to introduce the abbreviations  $v_{dt}$ -boost and  $i_{dt}$ -buck rectifier. Under omission of discussions of circuit details and derivations the operating properties of both systems are given and limitations inherent to the systems are pointed out.

## 2 Three-Phase Discontinuous Inductor Current Boost Rectifier – $v_{dt}$ -Boost Rectifier

Figure 7 shows the simplified structure of the power circuit of a three-phase  $v_{dt}$ -boost rectifier [10], [11]. For full controllability of the system the DC link voltage has to lie above the peak value of the line-to-line mains voltage under all circumstances. The turn-on interval of the power transistor and the pulse frequency  $f_P = 1/T_P$  of the system are constant during the fundamental period in the simplest case.

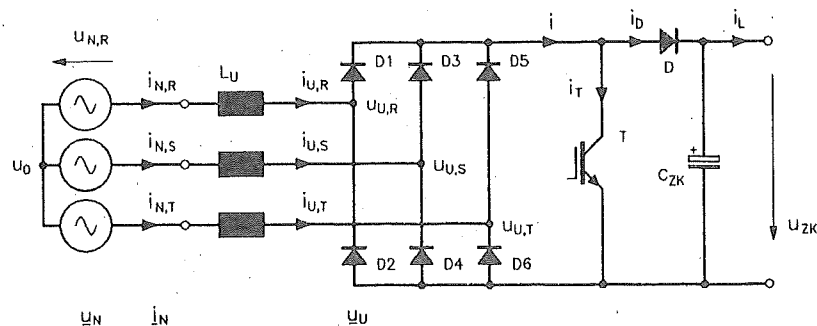
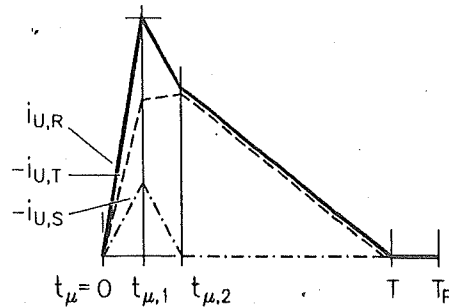
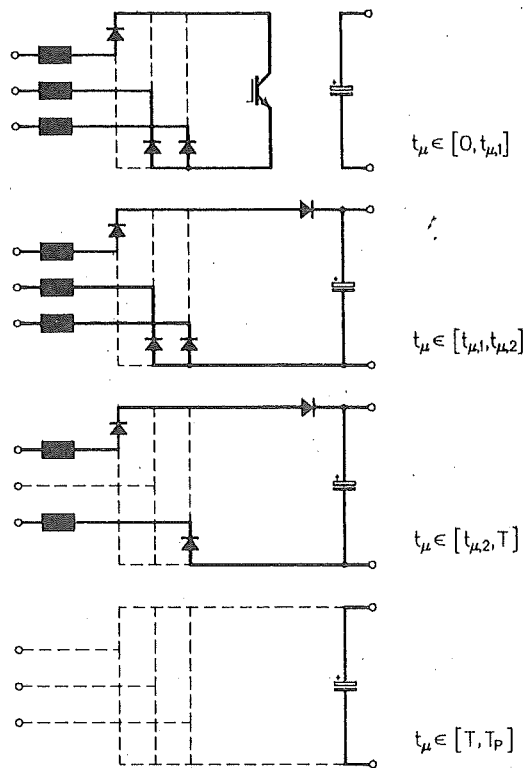


Fig.7: Simplified structure of the power circuit of a  $v_{dt}$ -boost rectifier. The supplying mains is substituted by a star connection of ideal voltage sources.

### 2.1 System Operation

The current generation on the AC side within a pulse period  $t_\mu \in [0, T_P]$  is shown in Fig.8. In the interval  $[0, t_{\mu,1}]$  the three-phase energy storage  $L_1$  on the input side is charged by the mains voltages. The discharge is performed in two discharging cycles  $[t_{\mu,1}, t_{\mu,2}]$  and  $[t_{\mu,2}, T]$ . Due to the high pulse frequency approximately triangular signal shapes result. The values of the phase currents obtained in  $t_\mu = t_{\mu,1}$  are proportional to the mains phase voltages. Therefore, in a first approximation, also the local average values of the phase currents show a shape proportional to the respective mains phase voltage. (These local average values are referred to a pulse period and determine the fundamental behavior.) After filtering of the input currents (not shown in Fig.7) we therefore obtain approximately ohmic mains loading. The power flow into the DC link is adjusted



**Fig.8:** Sequence of the conducting states and shape of the input phase currents within a pulse period  $0 \leq t_\mu \leq T_P$  for  $u_{N,R} > 0$ ,  $u_{N,T} \leq u_{N,S} \leq 0$ .  $[0, t_{\mu,1}] \dots$  turn-on interval of the power transistor T.

to the respective load conditions by the DC link voltage regulator via the turn-on interval of the power semiconductor. It has to be pointed out that the current flow is guided directly by the mains voltage and not, e.g., by sinusoidal variation of the duty ratio of the power transistor. Due to the triangular shape of the phase currents a stress on the transistor by reverse currents of the free-wheeling diode D is avoided. Therefore, one can reach a system pulse frequency lying above the audible spectrum.

## 2.2 Digital Simulation

For a clear representation of the operating principle of the pulse rectifier system in the following current and voltage shapes of a low-frequency pulsed  $v_{dt}$ -boost rectifier are given (cf. Fig.9). They are gained by digital simulation.

The mains phase current follows an envelope being proportional to the respective phase voltage. Therefore, in the mains current spectrum there appear especially components with switching frequency besides low-frequency current harmonics. The harmonics of the uncontrolled three-phase bridge (which are limited to the lower frequency region, cf. Figs.3, 4) are shifted to higher frequencies by pulsing. This results in a considerable reduction of the required filtering effort if the comparison is based on equal influence on the mains.

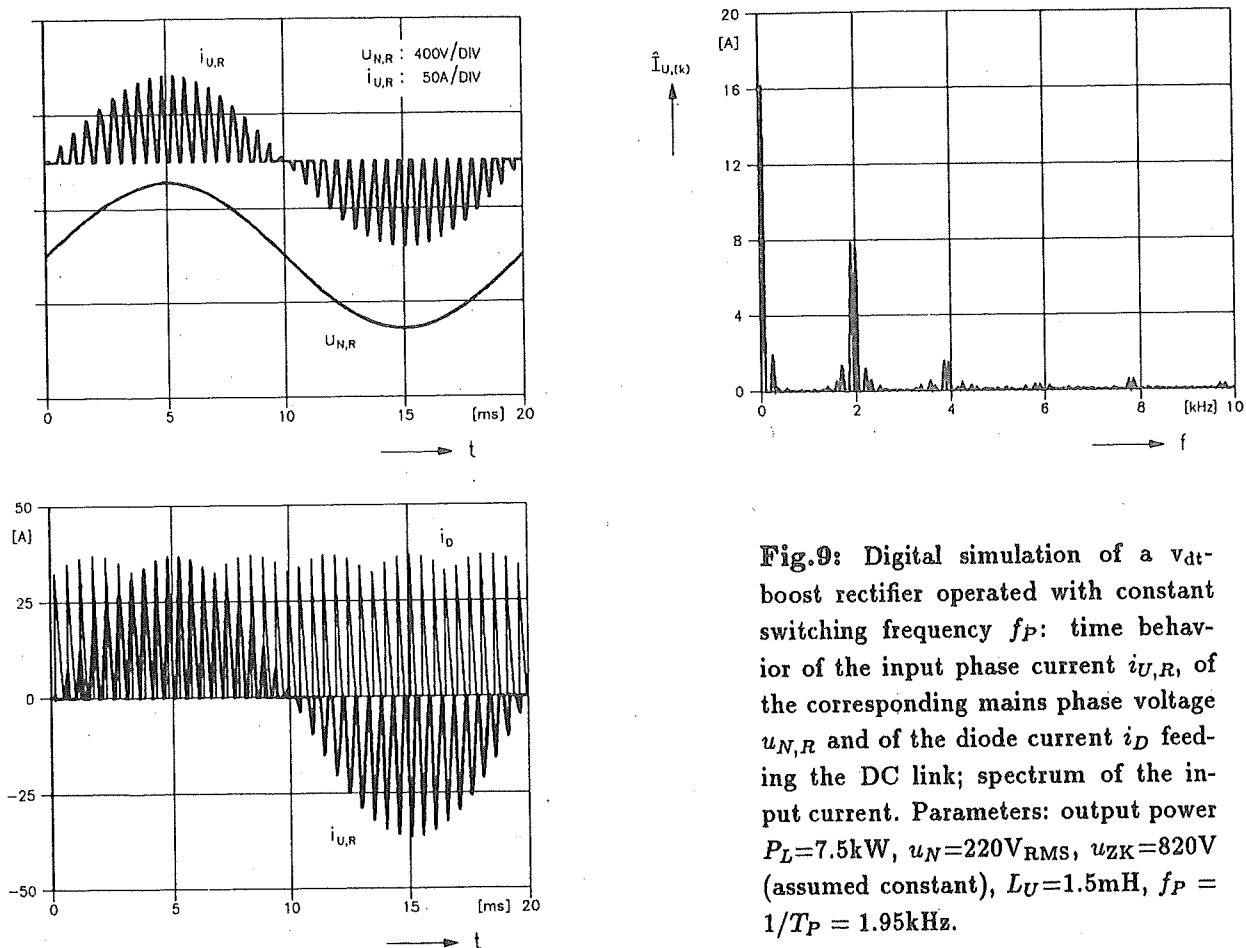


**Fig.9:** Digital simulation of a  $v_{dt}$ -boost rectifier operated with constant switching frequency  $f_P$ : time behavior of the input phase current  $i_{U,R}$ , of the corresponding mains phase voltage  $u_{N,R}$  and of the diode current  $i_D$  feeding the DC link; spectrum of the input current. Parameters: output power  $P_L=7.5\text{kW}$ ,  $u_N=220\text{V}_{\text{RMS}}$ ,  $u_{ZK}=820\text{V}$  (assumed constant),  $L_U=1.5\text{mH}$ ,  $f_P = 1/T_P = 1.95\text{kHz}$ .

### 2.3 Dimensioning of the Mains Filter

For avoiding loading of the mains by high-frequency current harmonics one has to extend the basic structure of a  $v_{dt}$ -boost rectifier (cf. Fig.7) by an input filter (cf. Fig.10). For dimensioning the filter devices the source impedance of the supplying mains has to be considered. The filter resonance frequency has to be set such that an excitation by ripple-control signals or by low-frequency current harmonics of the rectifier system can be avoided safely (cf. Fig.11, [12]). Also, sufficient damping of the current harmonics with switching frequency has to be obtained. This requires a sufficiently high converter pulse frequency.

### 2.4 Mathematical Analysis

#### 2.4.1 Space Vector Calculus

Due to its special clearness the space vector calculus is used for the mathematical analysis of the system behavior [13]. Considering the symmetries of a three-phase system the description can be limited to the interval  $[0, \pi/6]$  of the phase of the mains voltage space vector  $\underline{u}_N$  (cf. Fig.12).

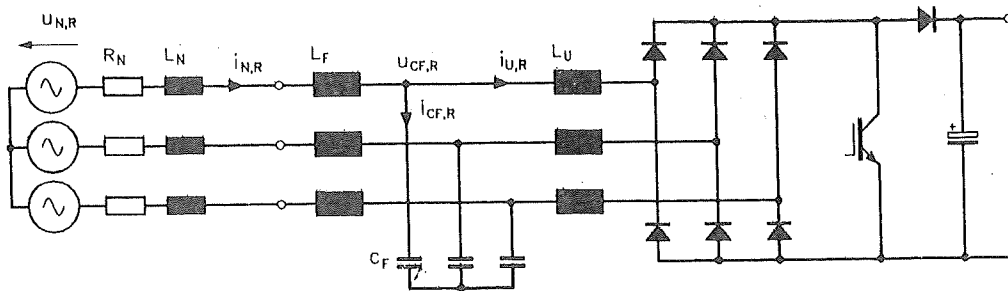


**Fig. 10:** Basic structure of the power circuit of a  $u_{d1}$ -boost rectifier for filtering of the rectifier input currents by a mains filter  $L_F$ ,  $C_F$ .  $R_N$  and  $C_N$  represent the equivalent circuit of the inner impedance of the supplying mains.

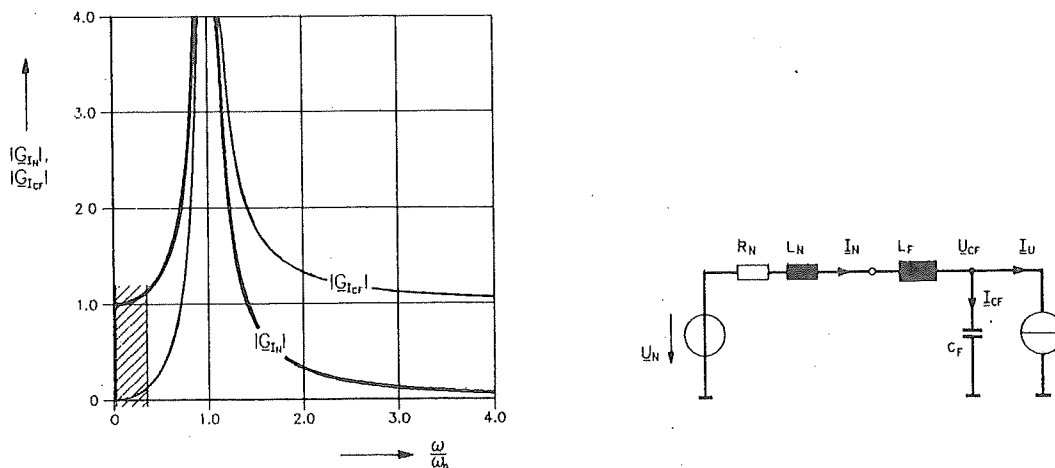


**Fig. 11:** Single-phase equivalent circuit of the AC side of the power electronic circuit shown in Fig. 10 and corresponding frequency behavior of the rated load of the mains  $|G_{I_N}| = |I_N|/|I_U|$  and of the filter capacitors  $|G_{I_{CF}}| = |I_{CF}|/|I_U|$  due to the impressed rectifier current  $I_U$ . For limiting the increase of low frequency harmonics of the converter current (hatched frequency area) in the mains current, the resonant frequency  $\omega_0$  of the filter has to be chosen appropriately high. On the other side, the converter operating frequency has to be sufficiently high to achieve a good damping of the switching frequency components of the converter current for the given  $\omega_0$  of the filter.

Within  $[0, t_{\mu,1}]$  the space vector of the converter input current  $i_U$  is built up in the direction of the mains voltage space vector. The demagnetization of the energy storing devices  $L_1$  is determined by the difference between mains and converter voltage space vector. Because in  $t_{\mu,2}$  the phase current  $i_{U,s}$  becomes 0, from here on only the projection of the demagnetizing voltage onto the line  $i_{U,s} = 0$  remains effective. This explains the deviation of the local shape of the converter phase currents (cf. Fig. 8) from the triangular shape.



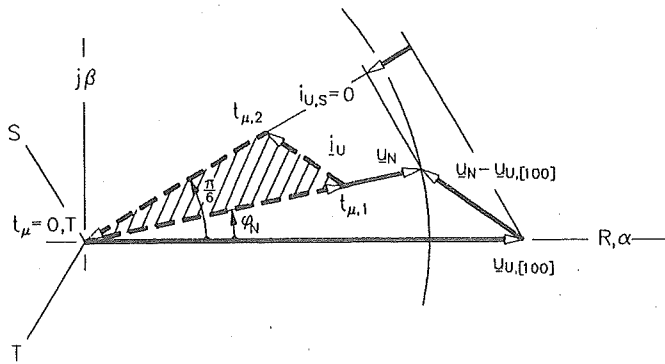


**Fig.12:** Description of the system operating principle by space vector calculus: trajectory of the input current space vector  $\underline{i}_U$  of a  $v_{dt}$ -boost rectifier within one pulse period  $0 \leq t_\mu \leq T_P$  for  $u_{N,R} > 0$  and  $u_{N,T} \leq u_{N,S} \leq 0$  (cf. Fig.8).  $\underline{u}_N$ : space vector of the mains voltages,  $\underline{u}_{U,[100]}$ : space vector of the rectifier input voltages when diodes D1, D4 and D6 are conducting.

### 2.4.2 Quasi-Continuous Analytical Approximation

Based on the previously given description of the local current and voltage generation, on the high pulse frequency and on averaging of the signal shapes over a pulse period one can calculate directly a sufficiently exact approximation of the mains current shape (filtered converter current) and of the mains current spectrum. This is especially of interest for determining the applicability of the pulse rectifier system. The mains current shapes resulting for different control methods are summarized in the next section.

## 2.5 Mains Current Shape — Control Methods

In the following approximations of the time behavior and of the low-frequency mains current harmonics of a  $v_{dt}$ -boost rectifier are given. Figure 13 shows the following control methods:

- (i): Switching frequency  $f_P$  and turn-on time  $t_{\mu,1}$  constant during the fundamental period (Fig.13, top; DC link power oscillations occurring due to low-frequency mains current harmonics are not controlled; the corner frequency of the DC link voltage control loop lies below six times the mains frequency);
- (ii): As (i), but  $f_P$  not constant (Fig.13, center). The power transistor is turned on again immediately after demagnetization of  $L_1$  in  $t_\mu = T$ . A pause with zero current  $t_\mu \in [T, T_P]$  is avoided;
- (iii): As (i), but turn-on time  $t_{\mu,1}$  not constant. By using a highly dynamic DC link voltage control a power flow on the DC side is enforced which is constant in the average within each pulse interval (Fig.13, bottom). There,  $t_{\mu,1}$  is varied appropriately by the DC link voltage controller. The mains current harmonics lying in the neighbourhood of the multiples of six times the mains frequency show equal amplitude and opposite sign in this case. Therefore, they do not appear as DC link current harmonics.

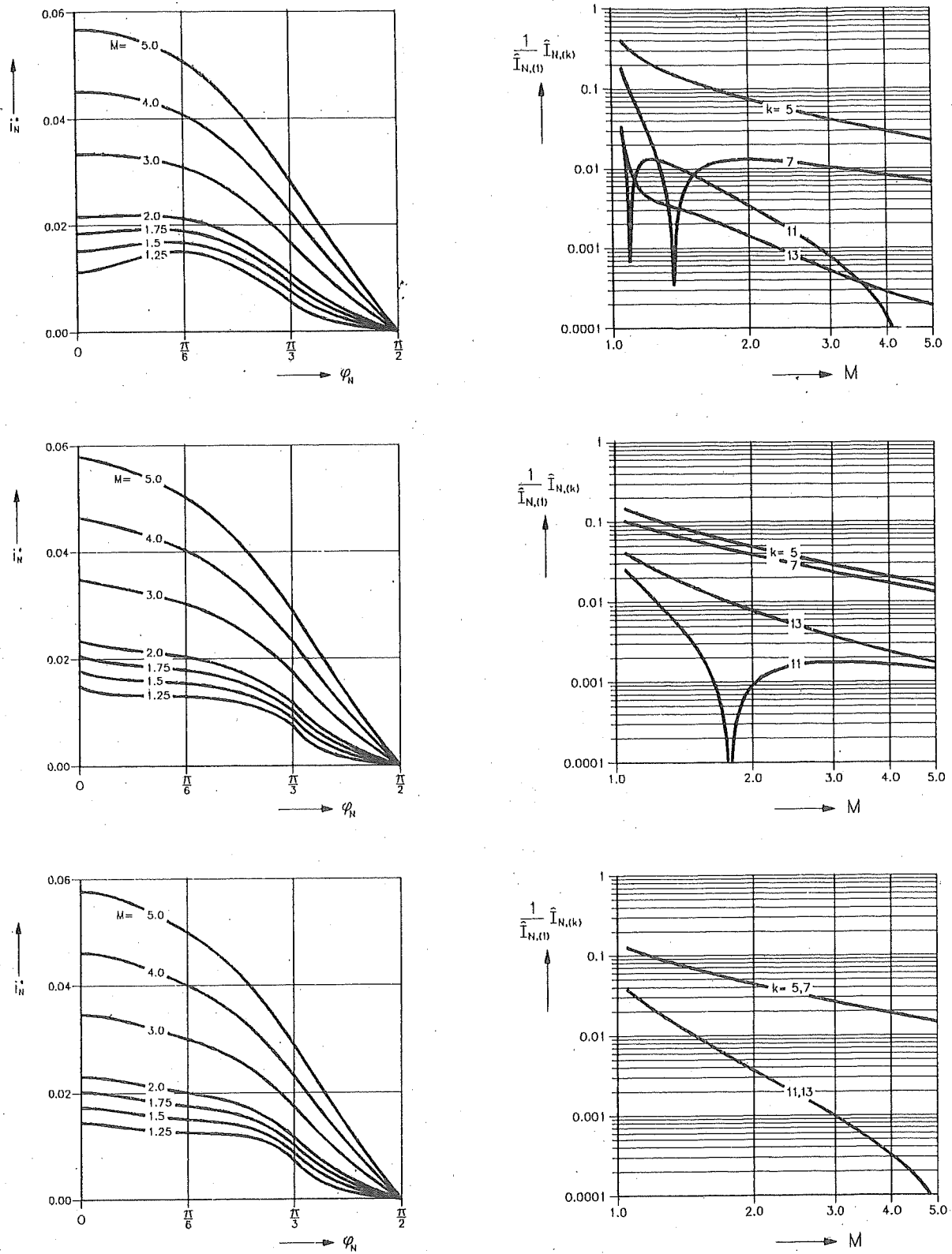


**Fig.13:** Comparison of different operating modes and control concepts of a  $v_{dt}$ -boost rectifier via illustrating the analytical computed time behaviors (given for a quarter of the fundamental period) and spectra of the mains current  $i_N$ . The curves are given for different voltage transformation ratios  $M = U_{ZK}/(\sqrt{3}\hat{U}_N)$  or for different order  $k$  of the (low frequency) harmonics, respectively.

As a more detailed calculation shows, the deviation from the exact values is limited to below 1% for pulse frequencies  $f_P \geq 200 \cdot f_N$  (i.e.,  $f_P = 10\text{kHz}$  for  $f_N = 50\text{Hz}$ ;  $f_N \dots$  frequency of the supplying mains).

For a practical system realization especially the control of the rectifier with constant  $f_P$  and a highly dynamic DC link voltage control is of importance (cf. Fig.13, bottom).

## 2.6 Experimental Results

The results of the theoretical considerations are verified by measurements on a laboratory circuit (cf. Fig.14). The comparison of Figs.6 and 14 shows especially clearly the linearization of the nonlinear characteristic of the uncontrolled three-phase bridge rectifier. The area enclosed by the dynamic characteristic of the pulse rectifier system is proportional to the reactive power of the fundamental as caused by the mains filtering [14].

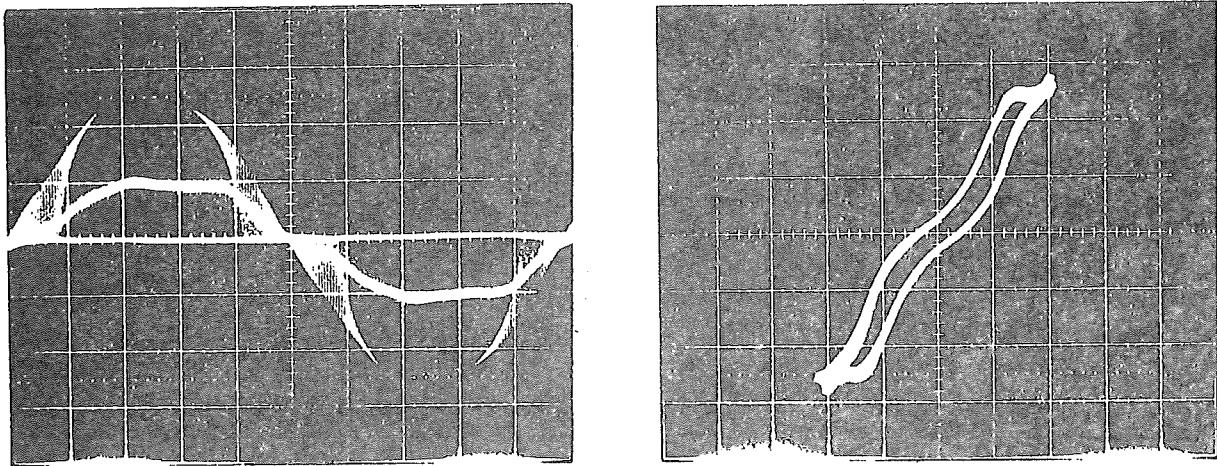
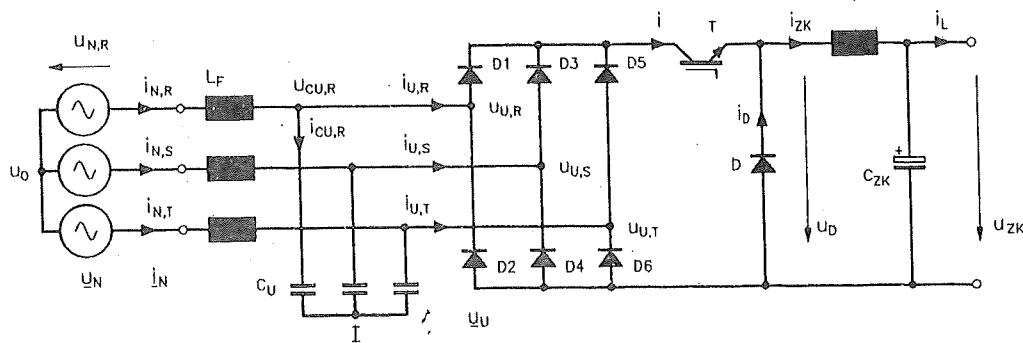


Fig.14: Measurements on a 2.5kW laboratory circuit of a  $v_{dt}$ -boost rectifier; left: time behavior of the input current and of the corresponding mains phase current; right: dynamic characteristic (horizontal axis: mains voltage, vertical axis: mains current). Parameters:  $M=1.25$ ,  $f_P=10\text{kHz}$ .

## 3 Three-Phase Discontinuous Input Capacitor Voltage Buck Rectifier – $i_{dt}$ -Buck Rectifier

As becomes immediately clear by simple duality considerations and as also mentioned initially, a linearization of the characteristic of a three-phase diode bridge besides high-frequency modulation of the DC side voltage can also be performed by high frequency modulation of the DC side current. The simplified structure of the resulting power electronic circuit is given in Fig.15. The upper limit of the obtainable DC link voltage is given by the peak value of the line-to-line mains voltage.



**Fig.15:** Simplified structure of the power circuit of an  $i_{dt}$ -buck rectifier. The supplying mains is replaced by a star connection of ideal voltage sources.

### 3.1 System Operation

For considering the system operating principle we will assume constant mains currents  $i_{N,RST}$  and a constant DC link current  $i_{zk}$  within a pulse period. An explanation of the system function can be omitted here due to the especially clear representation of the sequence of the conducting states of the converter (cf. Fig.16) and due to the quasi-dual relationship of the  $i_{dt}$ -buck and the  $v_{dt}$ -boost rectifier [15].

As the following calculations show, the shape of the capacitor voltage contains only small amplitudes of low-frequency harmonics. Therefore, again an approximately sinusoidal mains current shape is obtained. The high-frequency harmonics are filtered out by  $L_F$ .

### 3.2 Mathematical Analysis

#### 3.2.1 Space Vector Calculus

As a basis for the mathematical description of the system function one uses the space vector calculus again (cf. Fig.17). The considerations are limited to the interval  $[0, \pi/6]$  of the phase of the mains current space vector  $\underline{i}_N$ . These considerations are transferred to other angle regions by symmetry relationships.

#### 3.2.2 Quasi-Continuous Analytical Approximation – Stationary Operation – Initial Condition

Regarding the quasi-continuous approximation of the system behavior, the statements already made for the description of the  $v_{dt}$ -boost rectifier also are valid in this case. However, due to the higher system order, the stationary state of the converter can not be given directly. The determination of the stationary operating point is performed by a gradient method [16]. The output voltage is assumed to be constant. The initial value of the phase of the mains voltage space vector and the initial value of the magnitude of the mains current space vector and of the DC link current are guided into the stationary operating point based on the condition of  $\pi/3$ -symmetry of three-phase systems.

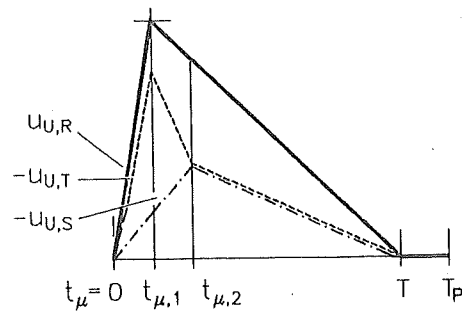
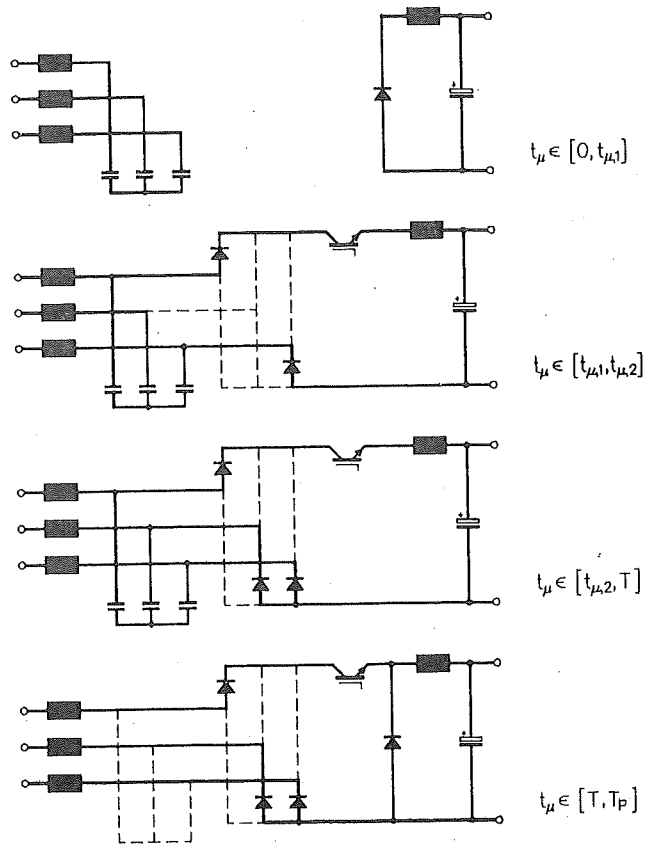


**Fig.16:** Sequence of the conducting states and shape of the input phase voltages  $u_{U,RST}$  of a  $i_{dt}$ -BR within a pulse period  $0 \leq t_\mu \leq T_P$  for  $i_{N,R} > 0$  and  $i_{N,T} \leq i_{N,S} \leq 0$ .  $[0, t_{\mu,1}]$  turn-off interval of the power transistor T.

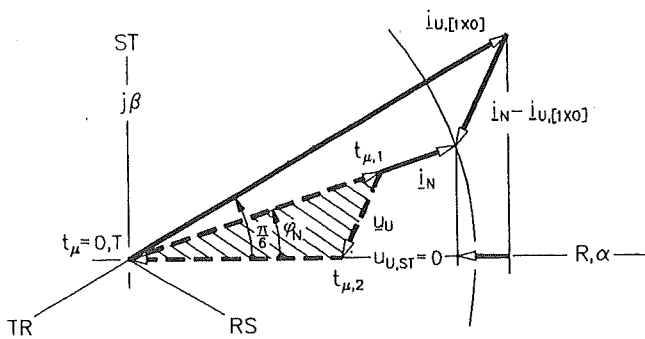


**Fig.17:** Description of the operating behavior of the system by space vector calculus: trajectory of the input voltage space vector  $\underline{u}_U$  of a  $i_{dt}$ -buck rectifier within a pulse period  $0 \leq t_\mu \leq T_P$  for  $i_{N,R} > 0$  and  $i_{N,T} \leq i_{N,S} \leq 0$  (cf. Fig.16);  $\underline{i}_N$ : space vector of the mains currents;  $\underline{i}_{U,[1x0]}$ : space vector of the rectifier input currents when diodes D1 and D6 are conducting (D3 and D4 are not conducting).

### 3.3 Mains Current Shape

According to Fig.18, the harmonic content of the mains current also in this case is determined by the ratio  $M$  between DC link voltage and peak value of the line-to-line voltage. If low stress on the mains due to harmonics is required, the application of the rectifier system has to be limited to the region  $M^{-1} \geq 2$ , therefore. (Then, the DC link voltage is  $\leq 270V$  for supply from the 380V three-phase system.)

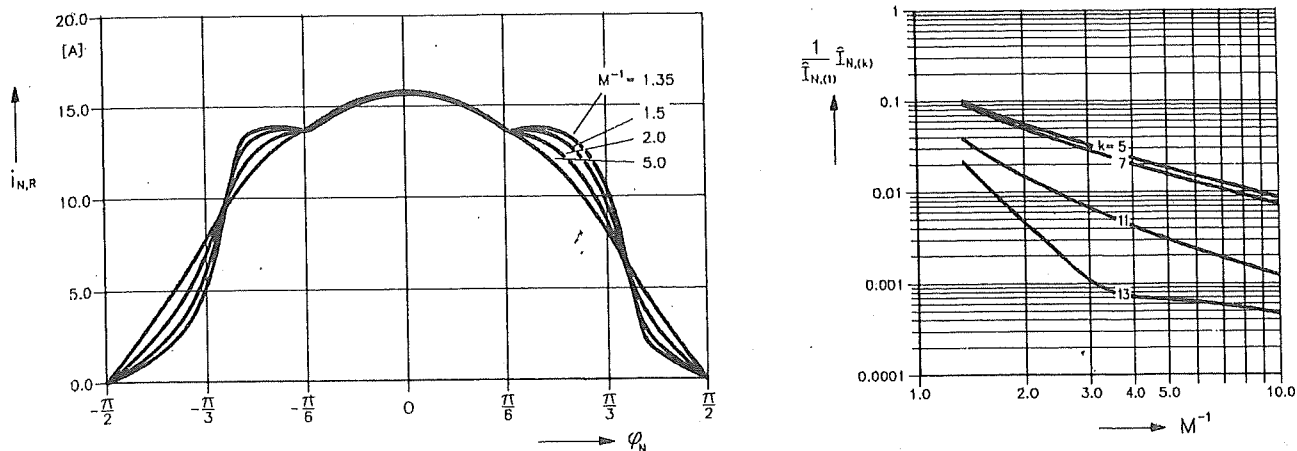


**Fig.18:** Comparison of the time behaviors (limited to a half period) and spectra of the mains currents  $i_N$  of an  $i_{dt}$ -buck rectifier for different values of the voltage transformation ratio  $M = U_{ZK}/(\sqrt{3}\hat{U}_N)$ . Parameter of the family of curves:  $M^{-1}$  or order  $k$  of the (low frequency) mains current harmonics.

#### 4 Further Converter Structures – Duality Relations – Converter Structures with Transformer Coupling

As Fig.19 shows, as an example, besides boost and buck converter also other basic DC/DC converter topologies [17] can be extended to current- or voltage-dither rectifier systems. These circuits, so far not given in literature, should gain more importance regarding the harmonic stress of the public low-voltage mains. This will be especially true when the relevant standards are made more stringent. Applications are, e.g., the supply of DC links of PWM converters for drives or electronic welding sources or (in connection with the application of "alternative" energy concepts) the realization of battery chargers with low influence on the mains.

If a potential separation between the mains side and the DC side is required, this can be achieved by using of a DC/DC converter pulsed with high-frequency connected in series. Also, for converters with capacitive energy transfer (Cuk, sepic, zeta) and for the buck-boost converter, this can be achieved without additional power semiconductors by inserting a two-winding transformer (cf. Fig.20).

A reduction of the blocking voltage stress on the power electronic devices on the DC side is given for cascading the output circuits of the pulse converters (cf. Fig.21). Therefore, IGBTs can be replaced by field effect transistors. This makes possible an increase of the pulse frequency reducing the filtering effort.

Finally it has to be pointed out that the introduced circuit concepts can be extended also to quasi-resonant operation by simple circuit modifications [18]. The relevant considerations are the object of further research work at present.

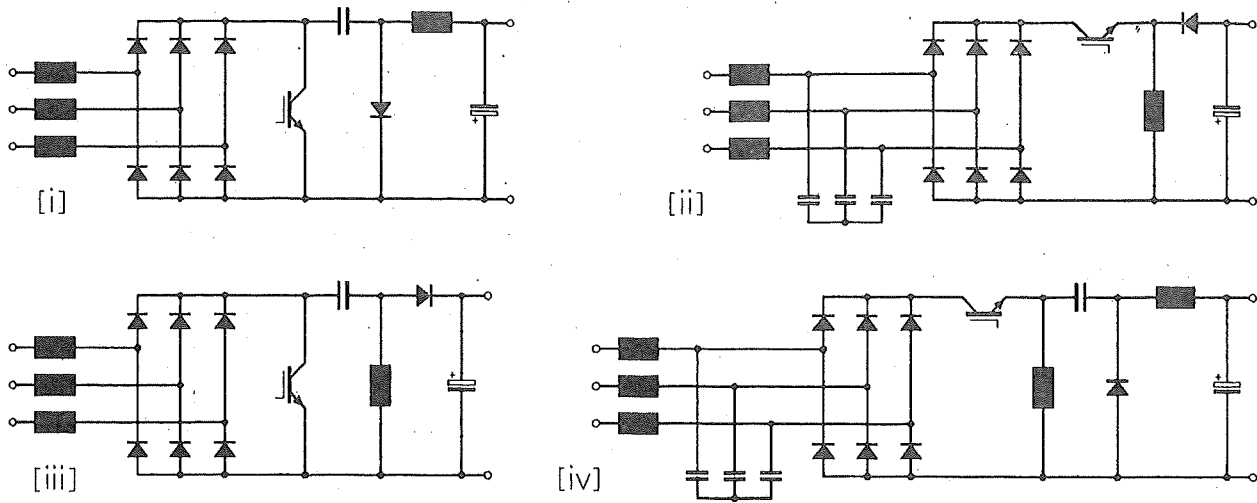


**Fig.19:** Structures of three-phase voltage or current dither rectifiers formed by an extension of basic DC/DC converter topologies. [i]:  $v_{dt}$ -Cuk rectifier, [ii]:  $i_{dt}$ -buck/boost rectifier (quasi-dual of [i]), [iii]:  $v_{dt}$ -sepic rectifier, [iv]:  $i_{dt}$ -zeta rectifier (quasi-dual of [iii]).

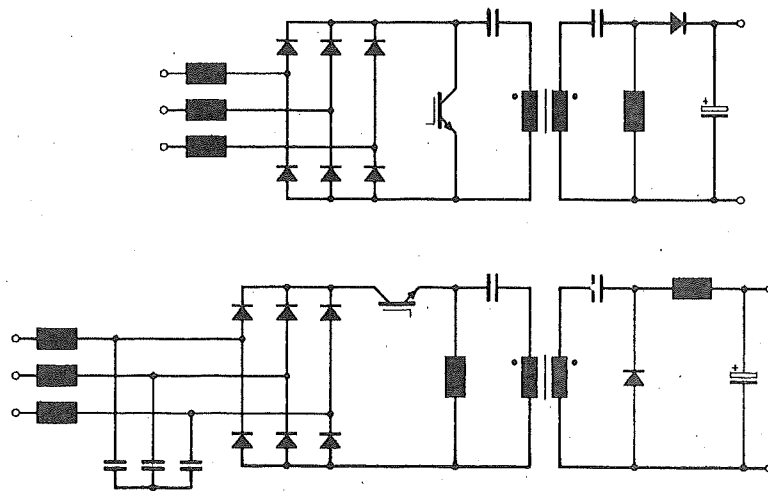


**Fig.20:** Transformer coupling of mains and DC side of three-phase voltage or current dither rectifiers shown by the example of a  $v_{dt}$ -sepic and an  $i_{dt}$ -zeta rectifier.

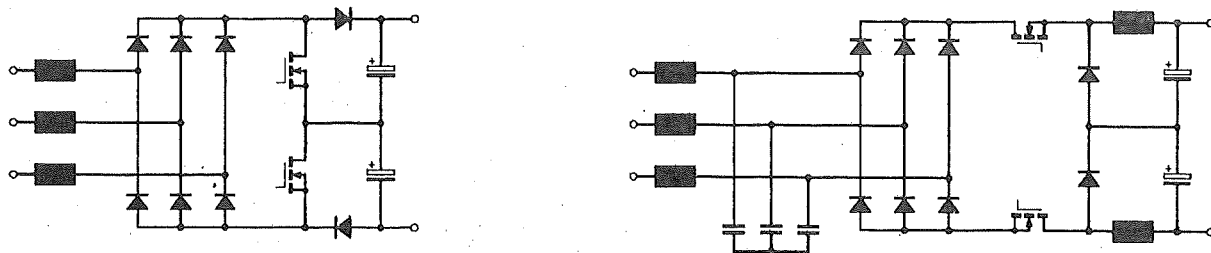


**Fig.21:** Cascading of three-phase voltage and current dither rectifiers; left: cascaded  $v_{dt}$ -boost rectifier; right: cascaded  $i_{dt}$ -buck rectifier. In both cases, the blocking voltage stress of the power transistors and of the output side diods is cut in half as compared to the simple converter structures (cf. Figs.7, 15).

## References

- [1] Gretsch, R.: *Messung und Berechnung von Netzurückwirkungen*. ETG-Fachbericht 17 - Netzurückwirkungen, Bremen, April 22-23, pp. 40-63 (1986).
- [2] Grötzbach, M., and Draxler, B.: *Line Side Behavior of Uncontrolled Rectifier Bridges with Capacitive DC Smoothing*. Conf. Record of the 3rd European Conference on Power Electronics and Applications, Oct. 9-12, Aachen, Germany, Vol. 2, pp. 761-764 (1989).
- [3] Hosemann, G., Kießling, G., and Meyer, W.: *Raumzeigerkomponenten bei Drehstrombrückenschaltungen*. etz-Archiv, Bd.7, H.3, pp. 95-98 (1985).
- [4] Takahashi, I.: *Power Factor Improvement of a Diode Rectifier Circuit by Dither Signals*. Conference Record of the 25th IEEE IAS Annual Meeting, Seattle, Oct. 7-12, Pt. II, pp. 1289-1294 (1990).
- [5] Zhang, H., and Mulhall, B.: *Implementation and Performance of a Reversible Rectifier*. Proceeding of the 24th PCIM Conference, Nürnberg, April 28-30, pp. 275-287 (1992).
- [6] Green, A. W., Boys, J. T., and Gates, G. F.: *Three-Phase Voltage Sourced Reversible Rectifier*. IEE Proceedings, Vol.135, Pt.B, No.6, pp. 362-370 (1988).
- [7] Katić, V. A., and Vučković, V. S.: *The Effects of Distorted Supply on PWM Rectifier AC Filter Design*. Proceeding of the 24th PCIM Conference, Nürnberg, April 28-30, pp. 219-229 (1992).
- [8] Koczara, W.: *Compensation in Demand for Drive Power*. Proceedings of the 6th Conference on Power Electronics and Motion Control, Budapest, Oct. 1-3, Vol.2, pp. 354-358 (1990).
- [9] Kolar, J. W., Ertl, H., and Zach, F.C.: *Realization Considerations for Unidirectional Three-Phase PWM Rectifier Systems with Low Effects on the Mains*. Proceedings of the 6th International Conference on Power Electronics and Motion Control, Budapest, Oct. 1-3, Vol.2, pp. 560-565 (1990).
- [10] Prasad, A. R., Ziogas, D., and Manias, S.: *An Active Power Factor Correction Technique for Three-Phase Diode Rectifiers*. IEEE Transactions on PE, Vol. 6, No.1, pp. 83-92 (1991).
- [11] Kolar, J. W., Ertl, H., and Zach, F.C.: *A Low-Cost Active Three-Phase Rectifier System*. Proceeding of the 24th PCIM Conference, Nürnberg, April 28-30, pp. 241-251 (1992).
- [12] Kloss, A.: *Oberschwingungen - Beeinflussungsprobleme der Leistungselektronik*. Berlin - Offenbach: VDE-Verlag, ISBN 3-8007-1541-4 (1989).
- [13] Jordan, K. R., Dewan, S. B., and Slemon, G. R.: *General Analysis of Three-Phase Inverters*. IEEE Trans. on Industry and General Applications, Vol. IGA-5, No.6, pp. 672-679 (1969).
- [14] Popescu, I. G., and Zaharia, I. C.: *Harmonic Power Flow in Nonlinear Circuits*. Proceedings of the 3rd International Power Quality Conference, Paris, Nov. 13-15, pp. 305-314 (1990).
- [15] Kolar, J. W., Ertl, H., and Zach, F. C.: *Analysis of the Duality of Three-Phase PWM Converters with DC Voltage Link and DC Current Link*. Conference Record of the IAS Annual Meeting, San Diego, Oct. 2-5, Vol.1, pp. 724-737 (1989).



- [16] von Lutz, R.: *Bestimmung des statischen und dynamischen Betriebsverhaltens von Stromrichterschaltungen*. Archiv für Elektrotechnik, Bd.70, pp. 39-48 (1987).
- [17] Liu, K.-H., and Lee, F. C.: *Topological Constraints on Basic PWM Converters*. Proceedings of the 19th PESC, Kyoto, Japan, April 11-14, pp. 164-172 (1988).
- [18] Pforr, J., and Hobson, L.: *A Three-Phase Pre-Converter for Induction Heating MOSFET Bridge Inverters*. Proceeding of the 24th PCIM Conference, Nürnberg, April 28-30, pp. 464-471 (1992).

#### ACKNOWLEDGEMENT

The authors are very much indebted to the Austrian FONDS ZUR FÖRDERUNG DER WISSENSCHAFTLICHEN FORSCHUNG which supports the work of the Power Electronics Section at their university.